THE JOURNAL OF PHYSICAL CHEMISTRY B

Article

pubs.acs.org/JPCB

Probing Dynamics and Mechanism of Exchange Process of Quaternary Ammonium Dimeric Surfactants, 14-*s*-14, in the Presence of Conventional Surfactants

Jun Liu,[†,‡] Yan Jiang,[†,∥] Hong Chen,[§] Shi Zhen Mao,*[,†] You Ru Du,[†] and Mai Li Liu*[,†]

[†]State Key Laboratory of Magnetic Resonance and Atomic and Molecular Physics, Wuhan Institute of Physics and Mathematics, Chinese Academy of Sciences, Wuhan 430071, P. R. China

[‡]Graduate University of Chinese Academy of Sciences, Beijing 100029, P. R. China

[§]State Key Laboratory of Oil and Gas Reservoir Geology and Exploitation, Southwest Petroleum University, Chengdu 610500, P. R. China

Supporting Information

ABSTRACT: In this Article, we investigated effects of different types of conventional surfactants on exchange dynamics of quaternary ammonium dimeric surfactants, with chemical formula $C_{14}H_{29}N^+(CH_3)_2-(CH_2)_s-N^+(CH_3)_2C_{14}H_{29}\cdot 2Br^-$, or 14-*s*-14 for short. Two nonionic surfactants, TritonX-100 (TX-100) and polyethylene glycol (23) laurylether (Brij-35), and one cationic surfactant, *n*-tetradecyltrimethyl ammonium bromide (TTAB), and one ionic surfactant, sodium dodecyl sulfate (SDS) were chosen as typical conventional surfactants. Exchange rates of 14-*s*-14 (s = 2, 3, and 4) between the micelle form and monomer in solution were detected by two NMR methods: one-dimensional (1D) line shape analysis and two-dimensional (2D) exchange spectroscopy (EXSY). Results show that the nonionic surfactants (TX-100 and Brij-35), the cationic surfactant (TTAB), and the ionic surfactant (SDS) respectively accelerated, barely influenced, and slowed the exchange rate of 14-*s*-14. The effect mechanism was investigated by the self-diffusion experiment, relaxation time measurements (T_2/T_1), the fluorescence experiment (I_1/I_3) and observed chemical shift variations. Results reveal that, nonionic conventional surfactants (TX-100 and Brij-35) loosened the molecule arrangement and decreased hydrophobic interactions in the micelle, and thus accelerated the exchange rate of 14-*s*-14. The cationic conventional surfactant (TTAB) barely changed the molecule arrangement and thus barely influenced the exchange rate of 14-*s*-14. The ionic conventional surfactant (SDS) introduced the electrostatic attraction effect, tightened the molecule arrangement, and increased hydrophobic interactions in the micelle, and thus slowed down the exchange rate of 14-*s*-14. Additionally, the two-step exchange mechanism of 14-*s*-14 in the mixed solution was revealed through interesting variation tendencies of exchange rates of 14-*s*-14.

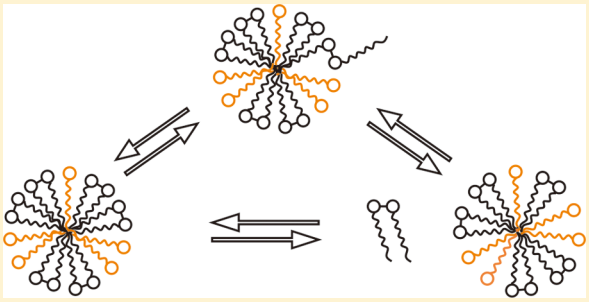

INTRODUCTION

Gemini surfactants are a new class of surfactants, containing two amphiphilic moieties connected at the level of head groups.[1] The gemini surfactants with chemical formula $C_mH_{2m+1}N^+(CH_3)_2-(CH_2)_s-N^+(CH_3)_2C_mH_{2m+1}\cdot 2Br^-$, or *m*-*s*-*m* for short (m and s are respectively the number of carbons of alkyl chains and linked groups), are a widely investigated type of quaternary ammonium dimeric surfactants. Gemini surfactants possess superior physicochemical properties compared to analogous conventional surfactants, such as better solubility and interfacial activity, lower critical micelle concentration (CMC) and Krafft temperature, and so on. In technological processes, they also exhibit more excellent performance properties involving foaming, emulsification, calcium-soap dispersion, and so on.[2,3]

As is well-known, surfactant molecules associate into micelles when the concentration of surfactants in the aqueous solutions is above the CMC. The micelles are in dynamic equilibrium with their monomers in the bulk solution. There are two relaxation processes in the micelle solutions: the τ_1 relaxation process (generally on the order of microseconds) and the τ_2 relaxation process (generally on the order of milliseconds).[4−6] In the τ_1 relaxation process, surfactant molecules quickly exchange between monomers in the micelles and those in the bulk solutions; in the τ_2 relaxation process, micelles constantly disintegrate and reform. The dynamic processes of micelles significantly influence the lifetime and stability of micelles, and thus largely affect technology processes.[7,8]

Mixed surfactants often show more distinguished properties than those attainable in their individual states. This phenomenon is called synergism.[9,10] Mixed surfactants are preferred as a result in practical application.[11,12] The properties

Received: August 20, 2012
Revised: November 28, 2012
Published: November 29, 2012

on the synergism of mixed surfactants based on Rubingh's theory were widely investigated.[13,14] Gemini surfactants were found to behave with greater synergism when mixed with conventional surfactants.[15] This feature of Gemini surfactants attracted people's interest. Much attention was given to the nonideality and synergism of mixed systems containing Gemini surfactants.[16−18] However, the kinetics of Gemini surfactant-containing mixed systems was less studied. The kinetics processes have a great effect on the technology process. So the study of kinetics of mixed surfactant systems containing Gemini surfactants is very important to achieve their better utilization.

The residence time of Gemini surfactants with long hydrophobic chains was found to be much longer than corresponding conventional surfactants by a factor about (10^3).[19,20] Ivan Huc and Reiko Oda[21] reported the slow exchange of 14-2-14 on the time scale of NMR, and obtained the exchange characteristic time through 1D line shape analysis, which proved NMR to be an effective tool to study the kinetics of Gemini surfactants. Afterward, Cui et al.[22] reported the slow exchange of 14-*s*-14 (s = 3 and 4) through 1D line shape analysis[23] and 2D EXSY[24] methods. Following the study of Cui et al.,[22] Jiang et al.[25] investigated the kinetics of 14-2-14 in the binary mixed solutions with different types of conventional surfactant. The results suggest that different types of conventional surfactant had different effects on the exchange rate of 14-2-14. Nevertheless, effects of conventional surfactants on the kinetics of 14-s-14 with (s = 3 and 4) were not investigated; particularly, the relationship between the effect and the spacer length (s) was undiscovered. Moreover, the effect mechanism ought to be further probed. In these respects, we will deeply study the kinetics of 14-*s*-14 (s = 2, 3, and 4) in binary mixed aqueous solutions with different types of conventional surfactants (TX-100, Brij-35, TTAB, and SDS) in this article.

EXPERIMENTAL SECTION

Figure 1 shows molecular formulas of 14-*s*-14 (s = 2, 3, and 4), TX-100, Brij-35, TTAB, and SDS and their proton numbering.

Materials. The quaternary ammonium gemini surfactants 14-*s*-14 (s = 2, 3, and 4) were synthesized and supplied by the Southwest Petroleum University. D_2O with a deuteration of 99.9% was a product of Cambridge Isotope Laboratories. TX-100, Brij-35, and SDS were respectively obtained from Nacalai Tesque, Trade (TCI) Mark, and Alfa Aesar. TTAB and pyrene were both obtained from Acros Organics. The reagents were used as received, without any further purification.

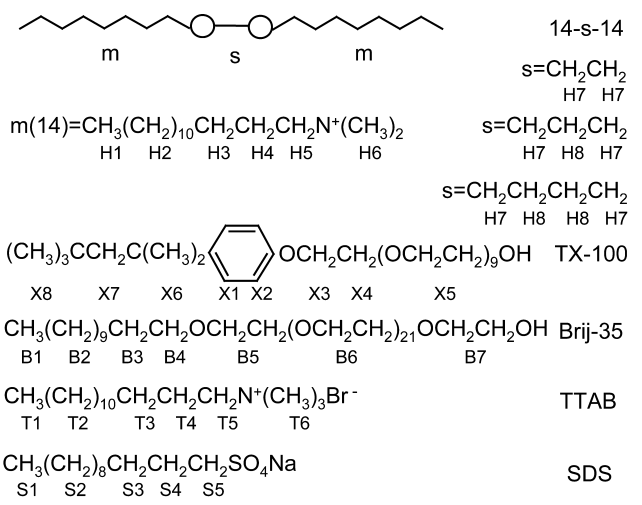

Figure 1. Molecular formulas and the proton numbering of surfactants 14-*s*-14 (s = 2, 3, and 4), TTAB, TX-100, Brij-35, and SDS.

Sample Preparations. Heavy-water solutions of 14-*s*-14, Brij-35, TX-100, and TTAB with a concentration of 1 mM were separately prepared. Then, binary mixed solutions of 14-*s*-14 to the other conventional surfactant with special mole ratios were compounded in EP tubes, and then every sample in each EP tube was gradually diluted into several concentrations. To make the samples dissolve more quickly and mix more homogeneously, an oscillator and an ultrasonic vessel were used. After the samples had been prepared, NMR experiments were made as described in the next section within a week in the case of coagulations.

Fluorescence Experiment. The fluorescence emission spectra were recorded using a Horiba Fluoromax-4 spectrofluorometer at 298 K, operated at an excitation wavelength of 335 nm, with a excitation slit of 5 nm and a emission slit of 1 nm. The concentration of pyrene for every solution was 10^{-6} mol/L.

NMR Experiment. All of the NMR measurements have been performed on a Bruker AVENCE-500 NMR spectrometer with a proton frequency of 500.13 MHz at 298 K. TSP_*d4* was used as the external reference. For the ^{1}H spectrum, a small-angle pulse of 30° was used rather than 90° in the conventional single-pulse sequence to save time. Also, presaturation was used to suppress the water signal.

The self-diffusion coefficients were measured by the longitudinal Eddy current delay sequence with bipolar pulse pairs. Spin−lattice and spin−spin times (T_1, T_2) were respectively measured by an inversion recovery method and Carr−Purcell−Meiboom−Gill pulse sequences. Two-dimensional exchange spectroscopy (2D EXSY) experiments were performed with the "noesygpphpr" sequence available within the software of the instrument, that is, a standard three-pulse sequence with gradient pulse, phase-sensitive spectra, and presaturation method to suppress the water signal. Thirty-two accumulations and a t_2 (F_2 dimension) × t_1 (F_1 dimension) = 2048 × 256 sampling data point array were used. The data point array F_2 (F_2 dimension) × F_1 (F_1 dimension) = 2048 × 512 was used in the Fourier transformation after zero filling. Several 2D EXSY experiments with varied mixing times were performed to obtain the optimum mixing time ($t_{m,\,opt}$).

1D Line Shape Analysis.[23] The characteristic time of exchange, τ, could be easily obtained through line shape analysis by

$$1/\tau = \pi\Delta\Delta\nu \tag{1}$$

where $\Delta\Delta\nu$ is the line width difference between the signal at a concentration of 14-*s*-14 twice its CMC and that at a concentration below the CMC (without exchange). $1/\tau$ was determined as the average exchange rate constant of 14-*s*-14.

2D EXSY Methods.[24] For an exchange system of two sites, A (monomers in bulk solutions) and B (surfactants in micelles), assumed as a pseudo-first-order reaction, one can write

$$\mathrm{A} \underset{k_{ba}}{\overset{k_{ab}}{\rightleftarrows}} \mathrm{B} \tag{2}$$

The dynamic process during the mixing time (t_m) can be expressed by the differential equation

dx.doi.org/10.1021/jp3082694 | J. Phys. Chem. B 2012, 116, 14859−14868

$$\frac{d}{dt}\mathbf{M} = \mathbf{L}\cdot\mathbf{M} \tag{3}$$

where

$$\mathbf{M} = \begin{pmatrix} M_a \\ M_b \end{pmatrix} \tag{4}$$

and

$$\mathbf{L} = \begin{pmatrix} -(k_{ab} + R_{1a}) & k_{ba} \\ k_{ab} & -(k_{ba} + R_{1b}) \end{pmatrix} \tag{5}$$

Here, $\mathbf{L}$ is the dynamical matrix, k is the exchange rate constant, and R_1 is the spin−lattice relaxation rate ($R_1 = 1/T_1$).

If the amplitude matrix $\mathbf{A}$ is defined as

$$\mathbf{A} = \mathrm{M}(t_m)\mathbf{M}_0^{-1} \tag{6}$$

$$\mathbf{M}_0 = \begin{pmatrix} I_{a0} & 0 \\ 0 & I_{b0} \end{pmatrix} \tag{7}$$

$$\mathbf{M}(t_m) = \begin{pmatrix} I_{aa} & I_{ab} \\ I_{ba} & I_{bb} \end{pmatrix} \tag{8}$$

Then the dynamical matrix $\mathbf{L}$ can be achieved, based on the well-known formula

$$\mathbf{L}t_m = \ln \mathbf{A} \tag{9}$$

Generally, it is simpler to expand ln $\mathbf{A}$ in a Taylor series:

$$\mathbf{L}t_m = \ln \mathbf{A} = (\mathbf{A} - 1) - \frac{1}{2}(\mathbf{A} - 1)^2 + \frac{1}{3}(\mathbf{A} - 1)^3 \cdots \tag{10}$$

The determination of $t_{m,opt}$ is achieved by processing several 2D EXSY experiments with various mixing times. For a two-site system, the optimum mixing time can be shown as

$$t_{m,opt} \approx (R_1 + k_{ab} + k_{ba})^{-1} \tag{11}$$

After the optimum mixing times, $t_{m,opt}$, had been determined, the exchange rate constants k_{ab} (the rate constant of monomers in the bulk solutions entering into micelles) and k_{ba} (the rate constant of monomers in the micelles exiting into the bulk solutions) of the exchange systems investigated at the individual optimum mixing time were obtained.

RESULTS AND DISCUSSION

1. Effects of Nonionic (TX-100 and Brij-35) and Ionic (TTAB and SDS) Conventional Surfactants on the Exchange Dynamics of 14-*s*-14 (*s* = 2, 3, and 4). Several mixed solutions at various ratios of conventional surfactant in each binary mixed system of 14-*s*-14 and the conventional surfactant were studied. The concentration of 14-*s*-14 in these mixtures was determined as 2CMC (within the concentration error of 10%) by comparing the integrals of resonance peaks of monomers in the micelle and in the bulk solution at the definite ratio.

1.1. 14-s-14/Nonionic Conventional Surfactants. The exchange rate constants, $1/\tau$ values, and k_{ab} and k_{ba} of 14-*s*-14 in the binary mixed micelle solutions of 14-*s*-14/TX-100 and 14-*s*-14/Brij-35 were quantitatively measured respectively by 1D line shape analysis and 2D EXSY. The results are listed in Tables 1 and 2, wherein the data of k_{ab} and k_{ba} of 14-2-14 in Table 2 are cited from ref 25. The results both suggest that changes of the exchange rates of 14-*s*-14 with s = 3 and 4 were similar to 14-2-14 reported by Jiang et al.[25] That is, the exchange rates of 14-*s*-14 were all accelerated by both TX-100 and Brij-35.

Table 1. Exchange Rate Constants, $1/\tau$, of 14-*s*-14 at Different Mole Fractions (α) of TX-100 and Brij-35 in Their Binary Mixed Solutions with the Concentration of 14-*s*-14 as 2CMC (Within the Concentration Error of 10%)

14-2-14		14-3-14		14-4-14	
$\alpha_{TX\text{-}100}$	$1/\tau(s^{-1})$	$\alpha_{TX\text{-}100}$	$1/\tau(s^{-1})$	$\alpha_{TX\text{-}100}$	$1/\tau(s^{-1})$
0	1.58	0	4.99	0	14.6
0.05	3.02	0.11	9.29	0.05	20.3
0.10	3.75	0.16	14.2	0.08	24.5
0.20	8.51	0.20	16.6	0.10	28.0
0.31	16.2	0.30	25.8	0.12	29.1
0.37	24.4	0.36	29.0	0.15	32.7
				0.18	34.7
				0.20	39.1
$\alpha_{Brij\text{-}35}$	$1/\tau(s^{-1})$	$\alpha_{Brij\text{-}35}$	$1/\tau(s^{-1})$	$\alpha_{Brij\text{-}35}$	$1/\tau(s^{-1})$
0	1.58	0	4.99	0	14.6
0.05	6.39	0.08	13.2	0.05	24.0
0.10	9.83	0.15	24.2	0.08	33.1
0.15	15.8	0.20	31.8	0.10	40.7
0.20	23.2	0.23	34.2	0.15	47.3
0.25	33.3	0.25	37.0	0.18	53.7

The variation tendencies of $1/\tau$ values of 14-*s*-14 with increasing mole fractions of TX-100 and Brij-35 are respectively displayed in Figure 2a,b. Also, exponential and linear functions were applied to fit the tendency. Both fitting results intuitively displayed the accelerating effects of TX-100 and Brij-35 on the exchange rate of 14-*s*-14. Additionally, the accelerating effect of Brij-35 is more distinct than that of TX-100, which is consistent to the result in the reported study.[25] Interestingly, the accelerating tendency of $1/\tau$ values of 14-*s*-14 with the shorter spacer length better accorded with exponential growth tendency, especially 14-2-14. However, the one with longer spacer length better accorded with linear growth tendency, especially 14-4-14. In short, the accelerating tendency of 14-*s*-14 went more obvious with the mole fractions of TX-100 and Brij-35 increasing, especially the one with shorter spacer length.

1.2. 14-s-14/Ionic Conventional Surfactants. The exchange rate constants, $1/\tau$ values of 14-*s*-14 in the binary mixed micelle solutions of 14-*s*-14/TTAB and 14-*s*-14/SDS, were quantitatively measured by 1D line shape analysis. The results are listed in Table 3. It suggests that the exchange rates of 14-*s*-14 changed little with increasing mole fractions of TTAB, but obviously slowed down with increasing mole fractions of SDS.

The variation tendency of $1/\tau$ values of 14-*s*-14 with increasing mole fractions of TTAB and SDS are respectively displayed in Figure 3a,b. Linear fitting results of variation curves of $1/\tau$ values in Figure 3a give very small linear coefficients less than 0.1. This suggests the little influence of TTAB on the exchange rate constants of 14-*s*-14 within the experiment error. The exponential and linear functions were also applied in Figure 3b. Both fitting results well displayed the decline tendency of $1/\tau$ values of 14-*s*-14 with increasing mole fractions of SDS. However, the variation tendency of $1/\tau$ values of 14-*s*-14 with the shorter spacer length better accorded with a linear decline tendency, especially 14-2-14. The one with longer

dx.doi.org/10.1021/jp3082694 | J. Phys. Chem. B 2012, 116, 14859−14868

Table 2. Exchange Rate Constants, k_{ab} and k_{ba}, of 14-*s*-14 at Different Mole Fractions (α) of TX-100 and Brij-35 in Their Mixed Solutions with the Concentration of 14-*s*-14 as 2CMC (Within the Concentration Error of 10%), Where the Data of 14-2-14/TX-100 and 14-2-14/Brij-35 Mixed Systems Are Cited from Ref 25

14-2-14[25]			14-3-14			14-4-14		
α_{TX-100}	$k_{ab}(s^{-1})$	$k_{ba}(s^{-1})$	α_{TX-100}	$k_{ab}(s^{-1})$	$k_{ba}(s^{-1})$	α_{TX-100}	$k_{ab}(s^{-1})$	$k_{ab}(s^{-1})$
0	1.14	1.93	0	5.11	5.59	0	14.9	18.3
0.12	6.07	6.21	0.11	8.32	9.48	0.05	20.5	24.4
0.18	6.70	8.20	0.20	12.6	20.2	0.08	20.4	29.0
0.28	9.83	13.7	0.30	23.0	29.8	0.10	28.1	33.1
			0.35	28.8	35.4	0.12	33.2	41.8
						0.18	34.8	48.1
						0.20	43.4	57.1
$\alpha_{Brij-35}$	$k_{ab}(s^{-1})$	$k_{ba}(s^{-1})$	$\alpha_{Brij-35}$	$k_{ab}(s^{-1})$	$k_{ba}(s^{-1})$	$\alpha_{Brij-35}$	$k_{ab}(s^{-1})$	$k_{ab}(s^{-1})$
0	1.14	1.93	0	5.11	5.59	0	14.9	18.3
0.09	5.99	10.6	0.08	12.5	14.8	0.05	23.9	29.8
0.14	11.4	17.7	0.15	21.1	23.8	0.08	38.1	35.3
0.21	16.1	20.7	0.23	25.1	33.2	0.10	44.5	42.4
0.33	23.1	34.0				0.15	55.4	61.4
						0.18	62.9	61.7

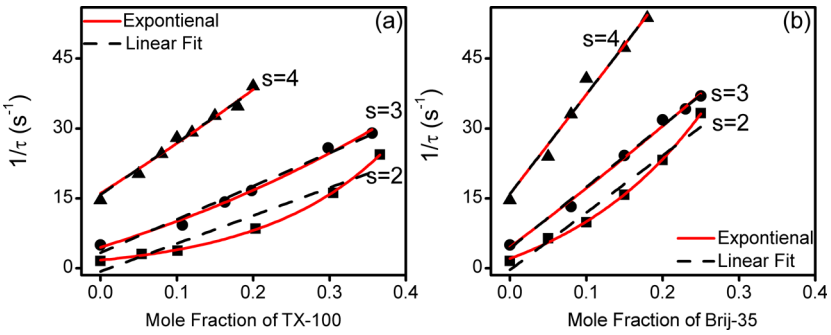

Figure 2. Variations of the exchange rate constant ($1/\tau$) of 14-*s*-14 with different mole fractions (α) of TX-100 and Brij-35 in their mixed solutions, where (a) and (b) respectively correspond to the 14-*s*-14/TX-100and 14-*s*-14/Brij-35 mixed systems.

Table 3. Exchange Rate Constants, $1/\tau$, of 14-*s*-14 at Different Mole Fractions (α) of TTAB and SDS in Their Binary Mixed Solutions with the Concentration of 14-*s*-14 as 2CMC (Within the Concentration Error of 10%)

14-2-14		14-3-14		14-4-14	
α_{TTAB}	$1/\tau(s^{-1})$	α_{TTAB}	$1/\tau(s^{-1})$	α_{TTAB}	$1/\tau(s^{-1})$
0	1.58	0	4.99	0	14.6
0.05	1.82	0.08	4.89	0.05	11.2
0.10	1.98	0.15	5.53	0.10	12.4
0.20	1.85	0.20	4.93	0.20	10.5
0.30	1.41	0.30	4.68	0.30	13.0
0.40	1.73	0.40	5.87	0.40	13.9
0.50	1.54	0.50	4.42	0.50	10.1
0.60	1.57	0.60	4.40	0.60	11.9
0.80	1.82				
α_{SDS}	$1/\tau(s^{-1})$	α_{SDS}	$1/\tau(s^{-1})$	α_{SDS}	$1/\tau(s^{-1})$
0	1.58	0	4.99	0	14.6
0.09	1.63	0.09	3.00	0.09	11.9
0.11	1.26	0.11	2.77	0.11	11.6
0.14	0.88	0.14	2.56	0.14	11.1
0.20	0.57	0.20	2.21	0.20	10.7

spacer length better accorded with an exponential decline tendency, especially 14-4-14.

The exchange rate ($1/\tau$) is directly related to the relaxation time constants (τ_1, τ_2) of the exchange dynamics, which highly influence the micellar stability and technological process.[7] So the results might be instructive to obtain a good usability of mixed surfactants containing gemini surfactants through choosing a proper formula and controlling the proportion.

2. The Mechanism of the Effect of Conventional Surfactants on the Exchange Kinetics of 14-*s*-14. Reported studies[6,19,20] show that the rate constant of entry of a surfactant into a micelle is close to one for a diffusion-controlled process, and the rate constant of exit from the micelle is highly dependent on the hydrophobicity of the surfactant. According to our previous work,[26] we know that binary mixed micelles formed when 14-*s*-14 mixed with TX-100, Brij-35, TTAB, and SDS in the solution. The microcosmic structure of the micelle was supposed to change as a result. It can be inferred that the electrostatic interactions in the headgroup and the hydrophobic interactions in the alkyl chain inside the micelle would be affected as a result, which would influence the exchange rate of 14-*s*-14 in the mixed solution. Taking these three aspects (the solution viscosity and electrostatic and hydrophobic interactions) in account, we investigated the mechanism of the effect of conventional surfactants on the exchange rate of 14-*s*-14.

2.1. Viscosity of the Mixed Solution. The self-diffusion coefficients of H_2O in the 14-2-14/TX-100, 14-2-14/Brij-35, 14-3-14/TTAB, and 14-3-14/SDS mixed solutions at various mixing ratios under current study were measured by NMR diffusion experiment. The values are around 2.03×10^{-9} $m^2 \cdot s^{-1}$

dx.doi.org/10.1021/jp3082694 | J. Phys. Chem. B 2012, 116, 14859−14868

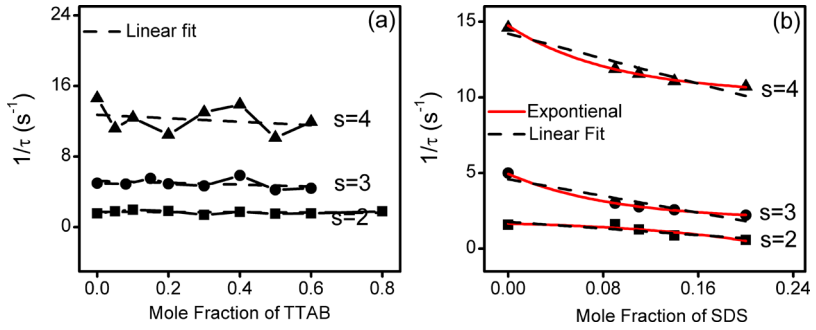

Figure 3. Variations of the exchange rate $(1/\tau)$ of 14-*s*-14 with different mole fractions (α) of TTAB and SDS in their mixed solutions, where (a) and (b) respectively correspond to the 14-*s*-14/TTAB and 14-*s*-14/SDS mixed systems.

Table 4. The Spin−Lattice and Spin−Spin Times (T_1 and T_2), Ratios of T_2/T_1 (T_R) of H6′, and I_1/I_3 Values in the Mixed Solutions of 14-2-14/TX-100, 14-2-14/Brij-35, 14-3-14/TTAB, and 14-3-14/SDS Mixed Systems

	14-2-14/TX-100					14-2-14/Brij-35			
$\alpha_{TX\text{-}100}$	T_1 (ms)	T_2 (ms)	T_2/T_1 (T_R)	I_1/I_3	$\alpha_{Brij\text{-}35}$	T_1 (ms)	T_2 (ms)	T_2/T_1 (T_R)	I_1/I_3
0	275	89	0.324	1.22	0	275	89	0.324	1.22
0.06	282	98	0.346	1.26	0.08	290	105	0.363	1.28
0.12	289	106	0.367	1.30	0.15	289	113	0.393	1.32
0.24	293	122	0.418	1.36	0.20	297	122	0.410	1.34
0.35	302	138	0.457	1.37	0.25	290	130	0.447	1.35
	14-3-14/TTAB					14-3-14/SDS			
α_{TTAB}	T_1 (ms)	T_2 (ms)	T_2/T_1 (T_R)	I_1/I_3	α_{SDS}	T_1 (ms)	T_2 (ms)	T_2/T_1 (T_R)	I_1/I_3
0	311	113	0.365	1.43	0	311	113	0.365	1.43
0.19	306	111	0.361	1.38	0.09	306	111	0.361	1.40
0.38	305	113	0.369	1.41	0.11	305	113	0.369	1.38
0.54	312	110	0.351	1.43	0.14	312	110	0.351	1.38
0.71	306	111	0.363	1.41	0.20	306	111	0.363	1.36

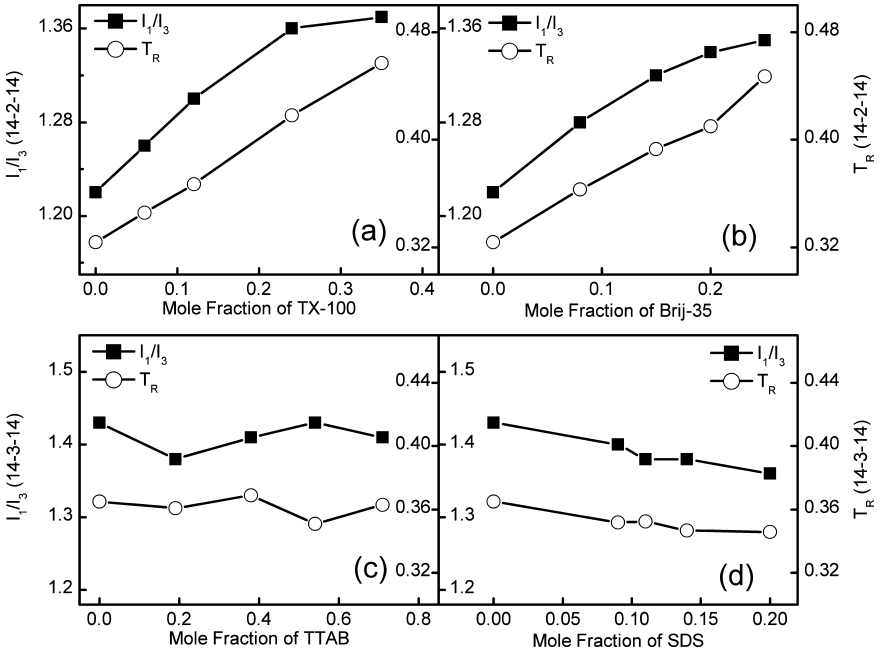

Figure 4. Variations of TR values for H6′ of 14-*s*-14 and I_1/I_3 values of pyrene with mole fractions of TX-100, Brij-35, TTAB, and SDS in the mixed solutions, where (a), (b), (c), and (d) repectively correspond to the mixed systems of 14-2-14/TX-100, 14-2-14/Brij-35, 14-3-14/TTAB, and 14-3-14/SDS.

with a standard error of not more than 0.02×10^{-9} $m^2 \cdot s^{-1}$, which can be considered within the experiment error. This suggests that the solution viscosity had changed little with the addition of TX-100, Brij-35, TTAB, and SDS. Thus the change of exchange rate of 14-*s*-14 could not result from the change of solution viscosity.

dx.doi.org/10.1021/jp3082694 | J. Phys. Chem. B 2012, 116, 14859−14868

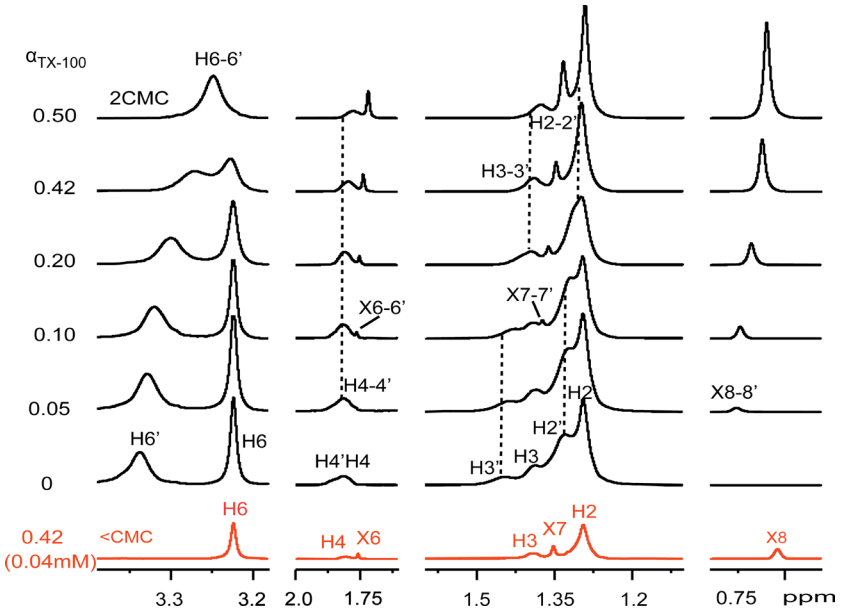

Figure 5. The selected 1H NMR spectra regions of 14-2-14/TX-100 mixed solutions at various mole fractions of TX-100 in D_2O at 25 °C, where the protons labeled Hn′, Hn-n′, and Xn-n′ are respectively the micelle resonance peaks and coalescence resonance peaks corresponding to the monomeric resonance peaks Hn of 14-2-14 and Xn of TX-100. The nethermost spectrum in the red color corresponds to the extremely diluted mixed solution.

2.2. Electrostatic and Hydrophobic Interactions in the Mixed Micelle.

2.2.1. Relaxation Measurement and Fluorescence Experiment. The spin−lattice and the spin−spin relaxation times (T_1, T_2) monitor molecule motions. The ratio of T_2/T_1 (T_R) gives a measure of the degree of departure of the molecular motion from the extreme narrowing condition.[27] T_R is unity for free molecule motion in the extreme narrowing condition. The deviation of the ratio from unity shows the motion restriction. H6′ corresponding to H6 is the resonance peak of protons in headgroup of 14-*s*-14 in the micelle state. It is the only singlet and nonoverlapped resonance peak in ^{1}H NMR spectra of the mixed micelle solution. Thus, T_R of H6′ can be used as a good probe to detect the microarrangement of the head groups in the mixed micelle.

The fluorescence technique can be used to study the micropolarity. Pyrene was solubilized in the micelle core in the surfactant micelle solution. After being excited at 335 nm, the fluorescence emission spectra of pyrene in aqueous solutions have five electronic vibration peaks. The intensity ratio of (I_1/I_3) in the first vibronic peak (around 373 nm) and the third vibronic peak (around 384 nm) is strongly dependent on the polarity of the environment of the pyrene molecules.[28] The I_1/I_3 value of pyrene is large in pure water (around 1.81 under current study). The value would drastically fall when pyrene is solubilized in the hydrophobic core of the micelle (around 1.20−1.43 under current study). The greater the hydrophobicity of the micelle core, the smaller the value of I_1/I_3. Thus pyrene can probe the microenvironment change of the hydrophobic core inside the micelle.

Table 4 listed the relaxation times T_1 and T_2, T_2/T_1 (T_R) of H6′ and I_1/I_3 values of pyrene in the 14-2-14/TX-100, 14-2-14/Brij-35, 14-3-14/TTAB, and 14-3-14/SDS mixed solutions. It is evident that T_R ratios of the proton H6′ in various mixed solutions are less than unity, as the motion is restricted in the micelle. Additionally, the I_1/I_3 values are much smaller than the one in pure water (1.81), which suggests that the pyrene molecule is solubilized in the micelle core. To clearly show the variation tendency of T_R and I_1/I_3, their variation curves are shown in Figure 4.

2.2.1.1. 14-s-14/Nonionic Conventional Surfactants. As shown in Figure 4a,b, in the 14-2-14/TX-100 and 14-2-14/Briij-35 mixed systems, T_R values of H6′ and I_1/I_3 values of pyrene apparently increased with growing mole fractions of TX-100 and Brij-35. This suggests that the motion restriction of head groups of 14-*s*-14 and the hydrophobicity inside the micelle core decreased with increasing mole fractions of TX-100 and Brij-35. The result indicates that the addition of TX-100 and Brij-35 into the mixed micelle may loosen the arrangement of molecules inside. The motion of head groups of 14-s-14 would be more flexible, and more water would penetrate into the micelle core. So the T_R values of H6′ and I_1/I_3 were observed to increase as a result. TX-100 and Brij-35 both have the headgroup of polyoxyethylene chain, which is much larger than that of a 14-*s*-14 molecule. The large head groups of TX-100 and Brij-35 may separate the ones of 14-*s*-14 further away and loosen the molecule arrangement inside the micelle.

2.2.1.2. 14-s-14/Ionic Conventional Surfactants. Figure 4c shows that, in the 14-3-14/TTAB mixed system, T_R values of H6′ and I_1/I_3 values of pyrene remain unchanged within the experiment error. This indicates that the motion restriction of head groups of 14-*s*-14 and the hydrophobicity inside the micelle core changed little with mole fractions of TTAB increasing. This result suggests that the addition of TTAB into the micelle may have little influence on the arrangement between the monomer chains of 14-s-14. This might be because TTAB has a similar molecular structure to 14-s-14, as it is the monomer conventional surfactant of 14-s-14.

Additionally, Figure 4d shows that, in the 14-3-14/SDS mixed system, T_R values of H6′ and I_1/I_3 values of pyrene obviously decreased with increasing mole fractions of SDS. This suggests that the motion restriction of head groups and the hydrophobicity inside the micelle core increased with the

dx.doi.org/10.1021/jp3082694 | J. Phys. Chem. B 2012, 116, 14859−14868

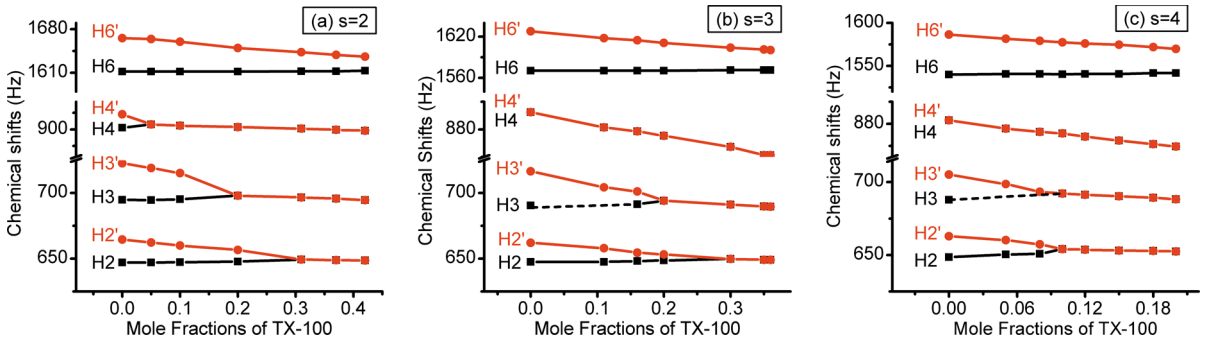

Figure 6. Chemical shift variations of protons at the 14-*s*-14 molecule in the micelle state with mole fractions of TX-100 in the 14-*s*-14/TX-100 mixed solution.

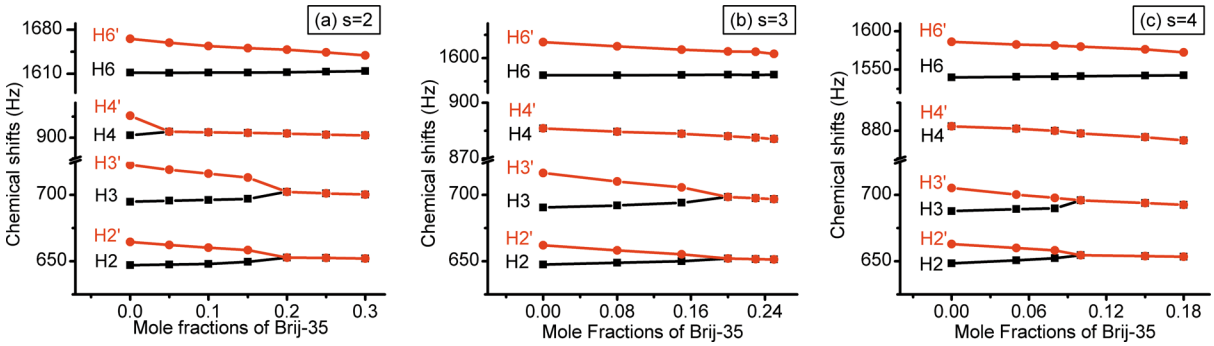

Figure 7. Chemical shift variations of protons at the 14-*s*-14 molecule in the micelle state with mole fractions of Brij-35 in the 14-*s*-14/Brij-35 mixed solution.

addition of SDS. The result indicates that the addition of SDS into the mixed micelle may tighten the arrangement of molecules inside. There exists electrostatic attraction between the sulfate headgroup of SDS and the quaternary ammonium headgroup of 14-s-14 in the mixed micelle after the addition of SDS. The electrostatic attraction effect may be a strong driving force to tighten the molecule arrangement in the micelle.

2.2.2. Observed Chemical Shift Variations. Changes in chemical shifts of proton resonance peaks may also reflect the variation in electrostatic and hydrophobic interactions between surfactant molecules in the micelle. For the protons in the molecule of 14-s-14, when the electrostatic and hydrophobic interactions they feel in the micelle increase, they will feel stronger Vander Waals effect and deshielding effect, and their chemical shifts would move to lower field. Otherwise, they move to higher field.

Benefit from the slow exchange process of 14-s-14 on NMR time scale, a set of micelle resonance peaks appear in the downfield separate from the ones of monomers in the bulk solution in ^{1}H NMR spectra, which are numbering as Hn′ corresponding to Hn. It has been shown in Section 1 that the slow exchange of 14-*s*-14 between monomers in the micelle and those in the bulk solution was gradually accelerated by the addition of TX-100 and Brij-35. When the exchange process becomes faster, the micelle resonance peaks (Hn′) and the monomer resonance peaks (Hn) of 14-*s*-14 come closer toward their center until they coalescence into a weighted one, which is labeled as Hn-n′ in the ^{1}H NMR spectra. The total concentrations of 14-*s*-14 in the binary mixed solutions in this Article are all 2CMC within 10% error. Thus, the chemical shifts of the weighted resonance peaks, $\delta_{Hn\text{-}n'} = (1/2)\,\delta_{Hn} + (1/2)\,\delta_{Hn'}$,[29] where, δ_{Hn} is deemed as changeless. So the variations of $\delta_{Hn\text{-}n'}$ in fact mirror the variations of $\delta_{Hn'}$ after the coalescence of Hn and Hn′ under current study. Thus, the variations of proton chemical shifts (Hn′, Hn-n′) of 14-*s*-14 in the mixed solutions are especially of concern in the ^{1}H NMR spectra to further investigate the change of electrostatic and hydrophobic interactions inside the micelle.

2.2.2.1. 14-s-14/Nonionic Conventional Surfactants. Figure 5 depicts the selected ^{1}H NMR spectra of the 14-2-14/TX-100 mixed solutions at various mole fractions of TX-100 in D_2O at 25 °C on behalf of 14-*s*-14/nonionic conventional surfactant mixed systems. The nethermost spectrum in the red color corresponds to the extremely diluted mixed solution of 14-2-14/TX-100.

It is evident that TX-100 and 14-2-14 molecules remain in monomeric states in the extremely diluted mixed solution with the fraction of TX-100 being 0.42 with the concentration of 14-2-14 being 0.04 mM, far below the CMC, where only the monomeric resonance peaks (Hn) appeared in the ^{1}H NMR spectrum. When the concentration of 14-2-14 reached 2CMC, the micelle resonance peaks (Hn′) appeared in the lower field. The chemical shifts of Hn′ all moved to higher field when TX-100 was added at a mole fraction of 0.054 with the concentration of 14-2-14 retained as 2CMC. Also H4′ and H4 obviously coalesced into a weighted peak H4−4′. The chemical shift of proton X8, located in the hydrophobic chain of TX-100 obviously moved to lower field at the concentration of TX-100 apparently below its individual CMC (0.3 mM[30]). It implies that the mixed micelle formed. As the exchange of TX-100 between the micelle and the bulk solution is fast on NMR time, the observed peaks of TX-100 are all weighted peaks in the mixed micelle solutions labeled as X*n*-*n*′. With the mole fraction of TX-100 increasing from 0.054 to 0.5, the exchange process of 14-*s*-14 molecules between the micelle and the bulk solution becomes fast. The micelle resonance peaks H6′, H3′,

dx.doi.org/10.1021/jp3082694 | J. Phys. Chem. B 2012, 116, 14859−14868

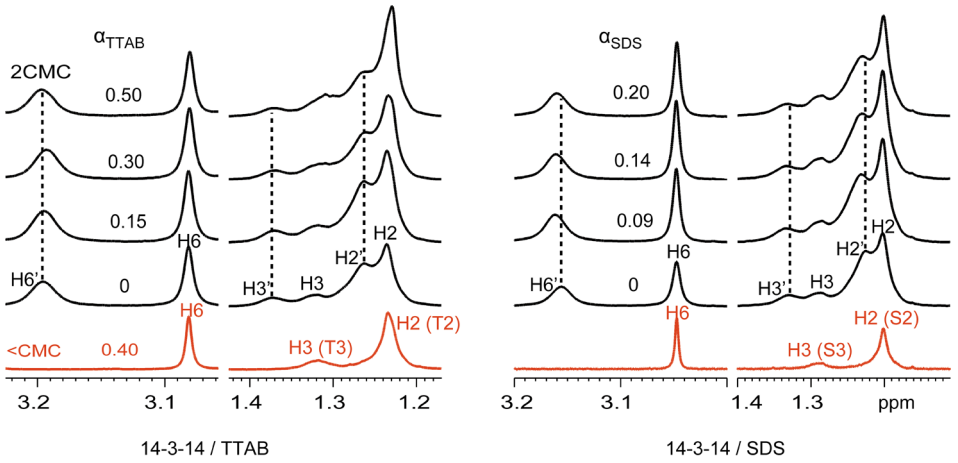

Figure 8. The selected 1H NMR spectra regions of 14-3-14/TTAB and 14-3-14/SDS mixed solutions at various mole fractions of TTAB and SDS in D2O at 25 °C. The protons labeled H*n*′ are the micelle resonance peaks corresponding to the monomeric resonance peaks H*n* of 14-3-14. The nethermost spectrum in the red color corresponds to the extremely diluted mixed solution.

and H2′ of 14-2-14 gradually moved to higher field, and their monomeric resonance peaks H6, H3, and H2 slightly move to lower field until they coalesce respectively into H6-6′, H3-3′ and H2-2′. Additionally, the coalesced peaks H4-4′, H3-3′, and H2-2′ continued to move to higher field. The exchange process accelerating will induce H*n* and H*n*′ to come closer in the same step. However, the tendency of H*n*′ to move to higher field is much more obvious than that of H*n* to move to lower field. This suggests that the chemical shift changes of H*n*′ are not only induced by the exchange process accelerating but also by the microcosmic environment change in the micelle. H6′ moving to higher field reflects that the electrostatic interactions felt by H6′ decreased with increasing mole fractions of TX-100. H2′ and H3′, and the coalesced peaks H4-4′, H3-3′, and H2-2′ moving to a higher field suggests that the hydrophobic interaction felt by protons in the alkyl chain of 14-*s*-14 in the micelle core also decreased.

In the 14-3-14/TX-100, 14-4-14/TX-100, and 14-*s*-14/Brij-35 mixed systems, proton chemical shifts of 14-*s*-14 have the same changes as the ones of 14-2-14 in the 14-2-14/TX-100 mixed system, respectively, with increasing mole fractions of TX-100 and Brij-35 (Tables S1 and S2). The chemical shift variation tendencies of 14-*s*-14 are shown in Figures 6 and 7. As shown, the micelle resonance peaks H*n*′ and their corresponding monomeric resonance peaks H*n* gradually coalesced with mole fractions of TX-100 and Brij-35 increasing as the exchange process accelerates. It is obvious that the tendency of H*n*′ moving to higher field is more obvious than that of H*n* moving to lower field. And the weighted coalescence peaks, H4-4′, H3-3′, and H2-2′ continued to move to higher field with increasing mole fractions of TX-100 and Brij-35. This suggests that the gradual insertion of Brij-35 and TX-100 into the mixed micelles of 14-*s*-14/TX-100 and 14-*s*-14/Brij-35, respectively, decreased the electrostatic interactions felt by protons in the headgroup and the hydrophobic interactions felt by protons in the alkyl chain of 14-*s*-14 inside.

This result is in good agreement with the one obtained from T_R and I_1/I_3 values in that the addition of TX-100 and Brij-35 into the micelle loosened the molecule arrangement. The electrostatic and hydrophobic interactions felt by 14-*s*-14 inside were supposed to decrease as a result. Additionally, the headgroup of TX-100 and Brij-35 added is noncharged, the addition of which into the micelle would certainly weaken the electrostatic repulsions felt by head groups of 14-*s*-14. The loosening of molecule arrangement and the weakening of hydrophobic interactions inside the micelle is supposed to reduce the energy barrier of the exchange process and accelerate the exchange rate of 14-*s*-14. Although the weakening of electrostatic repulsion felt by head groups of 14-*s*-14 is unfavorable to the accelerating of the exchange, the effect of the latter ones seems more obvious.

2.2.2.2. 14-s-14/Ionic Conventional Surfactants. Figure 8 depicts the selected ^{1}H NMR spectra regions of 14-3-14/TTAB and 14−3−14/SDS mixed solutions at various mole fractions of TTAB and SDS on behalf of the 14-s-14/ionic conventional surfactant systems. Similarly, the chemical shifts of micelle resonance peaks of 14-*s*-14 were concerned. As Figure 8 shows, all resonance peaks in the hydrophobic chains of TTAB (T1, T2, and T3) and SDS (S1, S2, and S3) molecules are in fact overlapped within the ones of 14-*s*-14 as they have similar alkyl chains to 14-*s*-14. In spite of that, the variations of chemical shift changes of 14-*s*-14 can still be reflected from the ^{1}H NMR spectra, as the signal intensities of TTAB and SDS are weak.

As Figure 8 shows, in the 14-*s*-14/TTAB binary mixed system, the chemical shifts of H6′, H3′, and H2′ were observed to barely move with increasing mole fraction of TTAB after the mixed micelle formed. This reflects that the electrostatic interactions felt by head groups and the hydrophobic interactions felt by the alkyl chain of 14-*s*-14 in the micelle have been changed little. This could be easily understood through the result from T_R and I_1/I_3 values that TTAB barely changed the molecule arrangement of the micelle. Additionally, TTAB has the same headgroup and the alkyl chain as 14-*s*-14. So its addition into the micelle would have little affect on the electrostatic and hydrophobic interactions felt by 14-*s*-14. Thus TTAB had little influence on the exchange rate of 14-*s*-14 in the mixed solution.

In the 14-*s*-14/SDS binary mixed systems, the chemical shifts of H6′, H3′, and H2′ were observed to obviously move to lower field when SDS was added into the mixed systems at its mole fraction of 0.09. This reflects that the protons in the headgroup and the alkyl chain of 14-s-14 respectively felt stronger electrostatic interactions and hydrophobic interactions as a result of the addition of SDS into the micelle. This result is understandable from the result of T_R and I_1/I_3 values in that SDS tightens the molecule arrangement of the mixed micelle.

dx.doi.org/10.1021/jp3082694 | J. Phys. Chem. B 2012, 116, 14859−14868

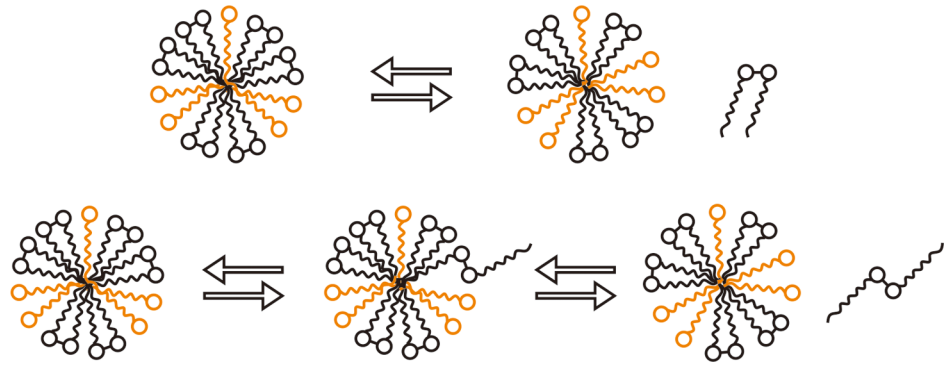

Figure 9. The scheme of a surfactant dimer molecule exchanging between the mixed micelle and the bulk solution.

The electrostatic and hydrophobic interactions felt by 14-*s*-14 in the micelle were supposed to increase as a result. Additionally, the sulfate headgroup has greater deshielding effect than the quaternary ammonium headgroup, the addition of which would also make H6′ feel greater deshielding effects and move to lower field. However, their chemical shifts changed little with the mole fraction of SDS increasing from 0.11 to 0.20. We guess that the change of the molecule arrangement in the mixed micelle becomes slight with mole fractions of SDS increasing so that the chemical shift variations cannot reflect it. The tightening of molecule arrangement and stronger hydrophobic interactions in the micelle would increase the energy barrier of the exchange process and slow the exchange rate of 14-*s*-14 in the mixed solution. Additionally, the strong electrostatic attraction between the head groups of 14-*s*-14 and SDS in the mixed micelle would also hinder the exchange process and slow the exchange rate of 14-*s*-14.

3. The Exchange Mechanism of 14-*s*-14 in the Mixed Micelle Solution. From Figures 6 and 7 we known that, in the 14-*s*-14/TX-100 and 14-*s*-14/Brij-35 mixed systems, the electrostatic and hydrophobic interactions of 14-*s*-14 in the micelle seemed linearly decreased with the mole fractions of TX-100 and Brij-35. In this respect, the exchange rate of 14-*s*-14 is supposed to accelerate in a linear tendency. However, Figure 2 shows an interesting accelerating tendency of the exchange rate of 14-*s*-14. That is, 14-*s*-14 with shorter spacer length, especially 14-2-14, better accord with an exponential tendency. A possible explanation is that 14-*s*-14 may adopt the two-step mechanism when there is exchange between the monomer in the micelle and the bulk solution. Large steric hindrance between the two adjacent chains of a surfactant dimer with short spacer length forces the dimer molecule to adopt a trans conformation. This results in the surfactant dimer molecule entering and exiting the micelle in a two-step process involving first one alkyl chain and then the other.[19] Figure 9 shows the scheme of two possible ways a dimer molecule, respectively adopting cis-form and trans-form, can exchange between the mixed micelle and the bulk solution.

The looseness effect on the rigidity of molecule arrangements in the micelle by TX-100 and Brij-35 weakens the hydrophobic interactions in the micelle on one hand, and promotes the conformational change of 14-*s*-14 in the exchange process on the other hand. The two effects both accelerate the exchange rate of 14-*s*-14. In the low mole fractions of TX-100 and Brij-35, the looseness effect on the rigidity is not so remarkable. The promotion of conformational change of 14-*s*-14 in the exchange process is not obvious. Only the weakening of hydrophobic interactions is dominant. With mole fractions of TX-100 and Brij-35 increasing, the extent of looseness effect on the rigidity of molecule arrangements enhances. The promotion of conformational change of 14-*s*-14 in the exchange process becomes more obvious. The accelerating extent of exchange rates of 14-*s*-14 is supposed to be larger than that at low mole fractions of TX-100 and Brij-35. So the accelerating tendency exhibits some exponential change as a result. With the spacer length of 14-*s*-14 decreasing, the steric hindrance between the adjacent chains increases, and so will the proportion of 14-*s*-14 in the trans conformation. Thus, 14-*s*-14 with the shorter spacer length exhibits more distinct conformational change in the exchange process. Therefore the accelerating tendency of 14-*s*-14 with shorter spacer length exhibited a more distinct exponential trend, especially 14-2-14 with the very short spacer length.

In the 14-*s*-14/SDS mixed system, the tightening effect of SDS on the molecule arrangement of the micelle seemed gradually slight with mole fractions of SDS. The slope of the decline tendency of the exchange rate of 14-*s*-14 is supposed to become smaller and smaller. Figure 3 depicts the good exponential decline tendency of 14-3-14 and 14-4-14 as expected. However 14-2-14 better accords with a linear decline tendency. This would also be understandable if the two-step mechanism of 14-*s*-14 molecule in the mixed solutions was taken in account. The tightening of molecule arrangement in the mixed micelle increases the electrostatic attraction effect and the hydrophobic interaction felt by 14-*s*-14 on one hand, and hinders the conformational change of 14-*s*-14 on the other hand. Also the hindrance effect becomes more obvious with the mole fraction of SDS increasing. This would enhance the slowing down effect of SDS on the exchange rate of 14-*s*-14 and makes the slowing tendency to exhibit a more obvious decline tendency than an exponential one at the large mole fraction. 14-2-14 exhibits more distinct conformational change in the exchange process than 14-3-14 and 14-4-14. In this respect, the exchange rates of 14-2-14 therefore exhibited a linear decline tendency different from the exponential decline tendency of 14-3-14 and 14-4-14.

■ CONCLUSIONS

We have investigated the effects of different kinds of conventional surfactants on quaternary ammonium dimeric surfactants, 14-*s*-14, in binary mixed micelle solutions. Results suggest that nonionic surfactants (TX-100 and Brij-35), the cationic surfactant (TTAB), and the ionic surfactant (SDS) respectively accelerated, barely changed, and slowed the exchange rate constant of monomers of 14-*s*-14 between the bulk solution and the micelle. This result would be instructive

to obtain a good usability when choosing a proper formula for the mixed surfactants. Additionally, the solution viscosity, molecule arrangement, and the electrostatic and hydrophobic interactions inside the mixed micelle were investigated to gain insight into the effect and exchange mechanism during the exchange process. Results reveal that the insertion of nonionic conventional surfactants (TX-100 and Brij-35) into the micelle of 14-s-14 loosened the arrangement of molecules and weakened the hydrophobic interactions felt by 14-*s*-14 in the micelle, and therefore accelerated the exchange rates of 14-*s*-14. The cationic conventional surfactant (TTAB) barely changed the arrangement among monomers and the electrostatic and hydrophobic interactions felt by 14-*s*-14 in the mixed micelle, and thus barely influenced the exchange rates of 14-*s*-14. The insertion of ionic conventional surfactant (SDS) into the micelle of 14-*s*-14 introduced the electrostatic attraction effect, tightened the molecule arrangement, and strengthened the hydrophobic interaction in the mixed micelle, and thus slowed the exchange rate of 14-*s*-14. The change of the accelerating and the decline tendencies of 14-*s*-14 with the spacer length revealed that 14-*s*-14 may adopt the two-step mechanism when exchange between the monomers in the bulk solution and the mixed micelle. In a word, this study would not only be instructive for better application but also would deepen our understanding of the dynamics mechanism of Gemini surfactants in mixed surfactant solutions.

■ ASSOCIATED CONTENT

Ⓢ Supporting Information

Corresponding proton chemical shift variations of 14-s-14 in the binary mixed solutions of 14-s-14/TX-100 at various mole fractions of TX-100 (Table S1); corresponding proton chemical shift variations of 14-s-14 in the binary mixed solutions of 14-s-14/Brij-35 at various mole fractions of Brij-35 (Table S2). This material is available free of charge via the Internet at http://pubs.acs.org.

■ AUTHOR INFORMATION

Corresponding Author

*E-mail address: maosz@wipm.ac.cn (S.Z.M.); ml.liu@wipm.ac.cn (M.L.L.). Tel.: 86-27-87197305; Fax: 86-27-87199291.

Present Address

[‖]Public Test Center, Chengdu Institute of Biology, Chinese Academy of Sciences, Chengdu 610041.

Notes

The authors declare no competing financial interest.

■ ACKNOWLEDGMENTS

Financial support by the National Science Foundation of China (2009CB918600, 20635040, 20975111, 20921004) is gratefully acknowledged.

■ REFERENCES

(1) Menger, F. M.; Littau, C. A. *J. Am. Chem. Soc.* **1993**, *115*, 10083−10090.
(2) Zana, R. *Adv. Colloid Interface Sci.* **2002**, *97*, 205−253.
(3) Rosen, M.; Tracy, D. *J. Surfactants Deterg.* **1998**, *1*, 547−554.
(4) Lang, J.; Tondre, C.; Zana, R.; Bauer, R.; Hoffmann, H.; Ulbricht, W. *J. Phys. Chem.* **1975**, *79*, 276−283.
(5) Aniansson, E. A. G.; Wall, S. N. *J. Phys. Chem.* **1974**, *78*, 1024−1030.
(6) Aniansson, E. A. G.; Wall, S. N.; Almgren, M.; Hoffmann, H.; Kielmann, I.; Ulbricht, W.; Zana, R.; Lang, J.; Tondre, C. *J. Phys. Chem.* **1976**, *80*, 905−922.
(7) Patist, A.; Kanicky, J. R.; Shukla, P. K.; Shah, D. O. *J. Colloid Interface Sci.* **2002**, *245*, 1−15.
(8) Groth, C.; Nydén, M.; Holmberg, K.; Kanicky, J.; Shah, D. *J. Surfactants Deterg.* **2004**, *7*, 247−255.
(9) Hoffmann, H.; Poessnecker, G. *Langmuir* **1994**, *10*, 381−389.
(10) Jost, F.; Leiter, H.; Schwuger, M. J. *Colloid Polym. Sci.* **1988**, *266*, 554−561.
(11) Rosen, M. *J. Am. Oil Chem. Soc.* **1989**, *66*, 1840−1843.
(12) El-Batanoney, M.; Abdel-Moghny, T.; Ramzi, M. *J. Surfactants Deterg.* **1999**, *2*, 201−205.
(13) Holland, P. M.; Rubingh, D. N. *J. Phys. Chem.* **1983**, *87*, 1984−1990.
(14) Rosen, M. J. *Langmuir* **1991**, *7*, 885−888.
(15) Rosen, M. J.; Zhu, Z. H.; Gao, T. *J. Colloid Interface Sci.* **1993**, *157*, 254−259.
(16) Alargova, R. G.; Kochijashky, I. I.; Sierra, M. L.; Kwetkat, K.; Zana, R. *J. Colloid Interface Sci.* **2001**, *235*, 119−129.
(17) Zhao, J.; Christian, S. D.; Fung, B. M. *J. Phys. Chem. B* **1998**, *102*, 7613−7618.
(18) Zana, R.; Lévy, H.; Kwetkat, K. *J. Colloid Interface Sci.* **1998**, *197*, 370−376.
(19) Ulbricht, W.; Zana, R. *Colloids Surf., A* **2001**, *183−185*, 487−494.
(20) Frindi, M.; Michels, B.; Levy, H.; Zana, R. *Langmuir* **1994**, *10*, 1140−1145.
(21) Huc, I.; Oda, R. *Chem. Commun.* **1999**, 2025−2026.
(22) Cui, X.; Yang, X.; Chen, H.; Liu, A.-h.; Mao, S.; Liu, M.; Yuan, H.; Luo, P.; Du, Y. *J. Phys. Chem. B* **2008**, *112*, 2874−2879.
(23) Ramey, K. C.; Louick, D. J.; Whitehurst, P. W.; Wise, W. B.; Mukherjee, R.; Moriarty, R. M. *Org. Magn. Reson.* **1971**, *3*, 201−216.
(24) Perrin, C. L.; Dwyer, T. J. *Chem. Rev.* **1990**, *90*, 935−967.
(25) Jiang, Y.; Lu, X.-Y.; Chen, H.; Mao, S.-Z.; Liu, M.-L.; Luo, P.-Y.; Du, Y.-R. *J. Phys. Chem. B* **2009**, *113*, 8357−8361.
(26) Cui, X.; Jiang, Y.; Yang, C.; Lu, X.; Chen, H.; Mao, S.; Liu, M.; Yuan, H.; Luo, P.; Du, Y. *J. Phys. Chem. B* **2010**, *114*, 7808−7816.
(27) Mao, S. Z.; Zhu, L. Y.; Wang, T. Z.; Li, M. Z.; Wang, E. J.; Miao, X. J.; Fang, X. W.; Yuan, H. Z.; Du, Y. R. *Colloid Polym. Sci.* **2002**, *280*, 90−94.
(28) Zana, R.; In, M.; Lévy, H.; Duportail, G. *Langmuir* **1997**, *13*, 5552−5557.
(29) Cui, X.; Mao, S.; Liu, M.; Yuan, H.; Du, Y. *Langmuir* **2008**, *24*, 10771−10775.
(30) Yuan, H. Z.; Zhao, S.; Cheng, G. Z.; Zhang, L.; Miao, X. J.; Mao, S. Z.; Yu, J. Y.; Shen, L. F.; Du, Y. R. *J. Phys. Chem. B* **2001**, *105*, 4611−4615.